International Journal of Mechanical Engineering and Robotics Research

ISSN 2278 – 0149 www.ijmerr.com
Vol. 1, No. 1, April 2012

Research Paper

CONFOCAL LASER SCANNING MICROSCOPY FOR CHARACTERISATION OF SURFACE MICRODISCONTINUITIES OF VITRIFIED BONDED ABRASIVE TOOLS

Krzysztof Nadolny[1]* and Wojciech Kaplonek[1]

*Corresponding Author: ***Krzysztof Nadolny,*** ✉ *krzysztof.nadolny@tu.koszalin.pl*

Confocal laser scanning microscopy is a relatively new, extremely dynamic and rapidly developing variation of classical confocal microscopy. Recently, within the technical disciplines related to mechanical engineering and material sciences, an increasing interest in this technique has been observed. Modern, highly-efficient, automated machining processes. Often make use of grinding wheels with vitrified bond. When such an abrasive tool is in operation, its active surface becomes worn and numerous defects appear, which are highly disadvantageous to the machining process. It is therefore necessary to have a precise assessment of the grinding wheel surface. This article demonstrates that such an assessment can be carried out using an advanced confocal laser scanning microscopy technique. The 3D laser measuring microscope LEXT OLS4000 by Olympus, utilised in this work, enabled the precise measuring of ceramic grinding wheels with a technical designation 1-35×20×10-CrA/F80J7V and visible microdiscontinuities shaped with an abrasive water-jet. An analysis of the measurement data obtained was carried out using OLS4000 2.1 and TalyMap Platinum 5.0 software. The results of this data included 2D surface images and maps, 2D profiles as well as 3D surface topographies with calculated parameters. These results also prove the high effectiveness and usability of, both, the experiments realized and the measurement method proposed. This method might complement, or extend, other methods that may be used in the diagnosis of abrasive tools.

Keywords: Confocal laser scanning microscopy, Microdiscontinuities, Pink fused alumina, Vitrified bonded abrasive tools, Grinding wheels

INTRODUCTION

Searching for better and more effective ways of assessing the surfaces of abrasive tools, scientists and constructors of measuring systems have been trying to adapt solutions that were primarily designed for other

[1] Department of Production Engineering, Faculty of Mechanical Engineering, Koszalin University of Technology, Raclawicka 15-17, 75-620 Koszalin, Poland.

purposes and used in different areas of science and technology. Examples of such solutions can be found in the advanced methods of non-invasive imaging related to nano- and micro-computed tomography (μCT) (Favretto, 2007; Midgley *et al.*, 2007; Cierniak, 2011; and Surhone *et al.*, 2011), which originated within, and are derived from, the classical computed tomography (Hsieh, 2003; Buzug, 2008; and Kalender, 2011) used in diagnostics of the human body. Using such classical methods in modern measuring technique has a far wider scope. For several years there has been an appreciable increase in the interest shown toward methods that use confocal microscopy (Conn, 2010), thus far, related mainly with the biological and medical sciences (Pawley, 2006; and Price and Jerome, 2011). This increased interest is as a direct result of the improved possibilities to obtain contour images for subsequent sections and to generate a 3D image of the examined object's surface, as well as to achieve high quality and high resolution image data with relatively short acquisition and processing time. From the point of view of imaging, confocal microscopy successfully fills the gap between the conventional wide-field light microscopy and Scanning Electron Microscopy (SEM), which makes it highly advantageous, offering great application possibilities.

One of the modern variations of classical confocal microscopy is Confocal Laser Scanning Microscopy (CLSM) (Claxton *et al.*, 2010; and Miller *et al.*, 2010). This technique was developed in the early 1980s and the term "confocal" was first used in a work (Brakenhoff, 1979). The first commercial laser microscope entered the market in 1987 (Amos and White, 2003; and Jones *et al.*, 2005). Today many international corporations within the measurement industry (e.g., Keyence, Leica, Olympus, Nikon, Carl Zeiss) manufacture microscopes of this type.

CLSM is the next step in the development of confocal microscopy techniques, which started with M. Minsky of Harvard University patenting a double-focusing stage scanning microscopy in 1957 (Minsky, 1957; Minsky 1988; and Clarke and Eberhardt, 2002). Modern CLSM, based on Minsky's idea, uses numerous modern solutions from the fields of optoelectronics, microelectronics and computer science. These include stable monochromatic laser light sources of great power, highly-efficient systems with scanning mirrors, high-capacity optical fibers, thin-layered dielectric coatings and new types of detectors, whose application has resulted in noise reduction. Combined with rapidly developing computer technology (a few-hundred times growth in the calculation power of computers, for example), the perfection of image display methods, new technologies for storing vast amounts of data and the development of new algorithms for digital image processing, the scope of fields and applications in which CLSM can be used has broadened significantly (Mahmoud *et al.*, 2003; Chen *et al.*, 2006; Evans and Donahue, 2008; and Miao, 2011).

In this work the Authors considered the possibility of using the CLSM technique in characterizing surface microdiscontinuities of abrasive tools made from PFA abrasive grains and vitrified bond. Microdiscontinuities are local discontinuities in the surface structure of

the abrasive tool that do not alter its macrogeometry. They usually adopt the form of grooves and pits with a regular lay-out. They may be shaped in special dressing procedures (Plichta and Bil, 1992; and Nadolny and Kaplonek, 2012) or by using high-pressure/ abrasive water-jets, for example. Application of grinding wheels with active surface microdiscontinuities influences the distribution of thermal-mechanical energy within the grinding zone in a positive way and contributes to better thermal regulation, wear product and machined material chip removal, as well as more efficient coolant delivery (Plichta and Bil, 1992). An advanced 3D laser microscope LEXT OLS4000 by Olympus was used during the experiments.

MATERIALS AND METHODS

The main goal of the experiments carried out, that are described in this paper, was to analyse the possibility of using the CLSM technique in measuring surface microdiscontinuities of abrasive tools. The experiments were realized according to the schedule outlined below, and which included four steps:

Step 1: Choice and preparation of samples for testing.

Step 2: Shaping the discontinuities on the Grinding Wheel Active Surface (GWAS).

Step 3: Measuring the surface topography of areas on the grinding wheels with visible microdiscontinuities.

Step 4: Analysis and interpretation of the measurement data obtained.

During the experiments a set of 5 samples were used, all in the form of small ceramic grinding wheels (1 referential grinding wheel + 4 grinding wheels with shaped microdiscontinuities) with the technical designation 1-35×20×10-CrA/F80J7V. All of the grinding wheels (marked: R – referential, 7, 12, 16 and 46) were made from PFA, provided by Graystar LLC (USA), by the Division of Fundamentals of Materials Science at the Institute of Mechatronics,

Table 1: General Characteristics of PFA

Name	Pink Fused Alumina
Synonyms	Chromium (Pink) Fused Alumina, Pink Fused Aluminum Oxide, Pink FA, Alodur Pink, CrA
Chemical name	Chromium Fused Aluminum Oxide
Basic minerals	α-Al_2O_3
Chemical composition andpercentage of elements*	Al_2O_3 (99.52%), Fe_2O_3 (0.05%), Na_2O (0.18%),Cr_2O_3 (0.25%)
Crystal size (μm)	600-1400
Grain sizes	F80**
Melting point	2050 °C
True density (g/cm³)	≥ 3.90
Bulk density (g/cm²)	1.5-1.95
Knoop hardness (Kg/mm²)	2200-2300

Note: * Chemical composition for low chromium grains, * according to FEPA 42-1:2006, ANSI B74.12 and ISO 8486-1:1996 standards.

Nanotechnology and Vacuum Technique, within Koszalin University of Technology. The general characteristics of the abrasive used is presented in Table 1, while the characteristics of the small ceramic grinding wheels used in the measurements are included in Table 2.

Table 2: General Characteristics of Grinding Wheels Used in the Experiments

Technical designation	1-35×20×10-CrA/F80J7V
Grinding wheel type	1 – flat grinding wheel
Dimensions	External diameter 35 mm; Height 20 mm; Internal diameter 10 mm
Abrasive grain type	Pink Fused Alumina (CrA)
Abrasive grain fracture	80
Hardness class	J
Structure No.	7
Volume of grains	48%
Volume of bond	10%
Volume of pores	42%
Bond	Vitrified (amorphous glass bond)
Modifications	Microdiscontinuities shaped on the grinding wheel active surface

To obtain the surface microdiscontinuities a hydro-jetting process was used on all the samples, except the referential sample. The OMAX® 55100 JetMachining Center by Omax (USA), designed for cutting with a water/abrasive water jet, was used for this purpose. In the case of the abrasive water-jet, an abrasive, commercially named Indian Garnet and produced by Opta Minerals Inc. (Canada), was used.

Three microdiscontinuities in the form of grooves were shaped on the active surface of each sample. The depth of the jet input for the first groove was 0.563 mm. Each subsequent input was a doubled value of the previous one, and was respectively: 1.126 mm and 1.689 mm. The groove shaping time was constant, lasting 5 seconds. The conditions and parameters for the process of shaping the surface microdiscontinuities with a water-jet and a

Table 3: Conditions and Parameters of the Abrasive Water-Jet and Water-Jet Processing

Lp.	Sample Designation	Processing	Type of Abrasive	Jewel (Orifice) Diameter (mm)	Mixing Tube Diameter (mm)	Abrasive Flow Rate (Kg/min)	Pressure (MPa)
1	R	–	–	–	–	–	–
2	7	Abrasive Water-Jet	Indian Garnet 80*	0.355	0.762	0.336	366.801**
3	12	Water-Jet	–	0.355	0.762	0.336	366.801**
4	16	Abrasive Water-Jet	Indian Garnet 80*	0.355	0.762	0.336	124.105***
5	46	Water-Jet	–	0.355	0.762	0.336	124.105***

Note: * Grit size: 80, ** pressure at nozzle in high pressure mode, *** pressure at nozzle in low pressure mode.

abrasive water-jet are presented in Table 3, while Figure 1 depicts the general view of the sample and the way in which the microdiscontinuities were shaped on its active surface.

Figure 1: The Process of Hydro-Jetting Samples, for the Obtaining of Surface Microdiscontinuities (a) General View of 1-35×20×10-CrA/F80J7V Grinding Wheel, (b) Diagram Showing the Way in Which the Microdiscontinuities were Forming on the Surface of the Grinding Wheel, and (c) Sample with Shaped Microdiscontinuities Fixed in Holder of OMAX® 55100 JetMachining Center

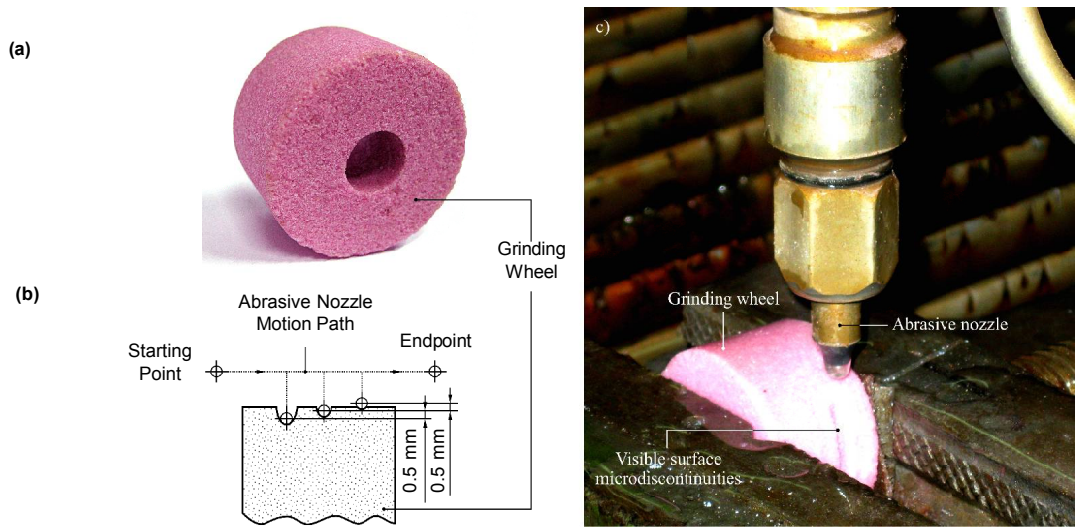

When the process of shaping microdiscontinuities on the GWAS was completed, they were thoroughly assessed. An advanced 3D laser measuring microscope, LEXT OLS4000 by Olympus (Japan), was used for this purpose. A general view of the microscope is presented in Figure 2.

Figure 2: The Advanced 3D Laser Measuring Microscope LEXT OLS4000 Produced by Olympus, Which was Used During the Experiments Conducted

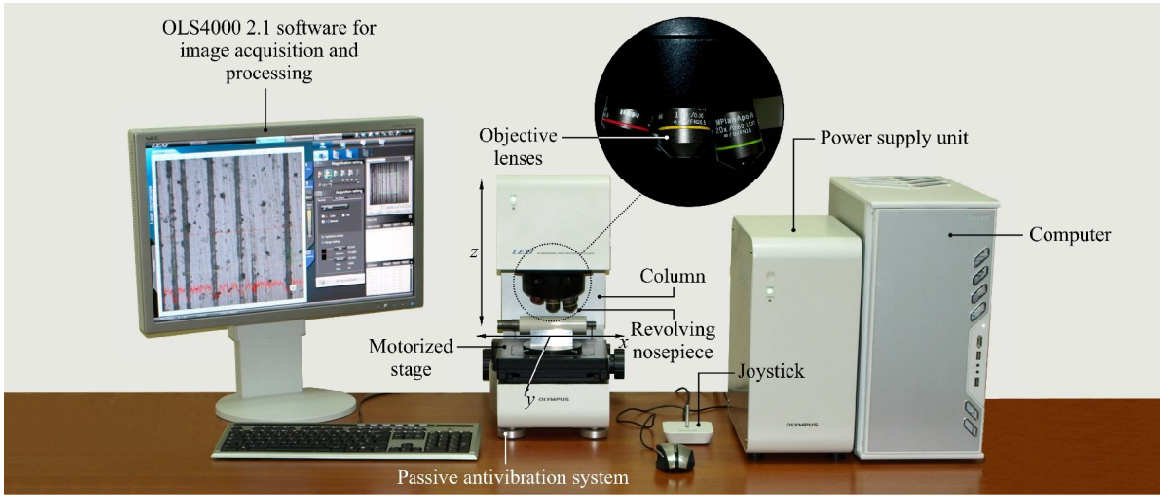

The advanced 3D laser measuring microscope LEXT, enabled the acquisition of images of the examined abrasive tools surfaces in two modes – microscopic and confocal one.

In the microscopic mode the examined sample was illuminated with light of a wavelength λ ranged 400-700 nm. An electroluminescent diode (LED), with 30 mW of power, was the light source. Four observation techniques were available in this mode: brightfield, darkfield, simple polarization and Differential Interference Contrast (DIC).

The operation of LEXT OLS4000 in the confocal mode consisted in generating an image on the basis of light reflection from the discrete focal plane. The light, creating an image with different focusing depth, was eliminated using the double confocal pinhole aperture. In this mode the microscope used a light beam with wavelength $\lambda = 405$ nm (violet), and the light source was a LED, with 120 mW of power. Obtaining a spatial mapping of the examined object's surface entailed its precise scanning, point by point on axes *x-y*. This process was realized by a special scanner patented by Olympus. The scanner used a Micro Electro-Mechanical System (MEMS). The images were acquired using a system of two photomultipliers, with average (standard) and high sensitivity. Such a system enabled proper amplification of the optical signal. Therefore it allowed for measuring the surfaces of elements with a low reflection coefficient and large surface slope angle, up to 85 degrees. The motorized revolving nosepiece included a set of 5 microscopic lenses with various magnification ranges (5×, 10×, 20×, 50×, 100×). The maximum magnification that could have been obtained was 17280×. The samples were placed on a motorized stage that allowed for precise realization of displacement on axes *x-y* (range: 100 mm) and axis *z* (range: 10 mm).

Regardless of the image acquisition mode, image processing and analysis was carried out using the dedicated OLS4000 2.1 software, provided by the microscope producer. The software offered numerous useful functions that proved helpful in the analysis of the abrasive tools surfaces. These were functions connected with: the measuring of geometrical parameters, quantitative analysis, detection of edges and surface roughness measurements. In this last case the program allowed for determination of over 80 surface roughness parameters, including amplitude, functional and volumetric ones. OLS4000 2.1 was supported with TalyMap Platinum 5.0 software, using Mountains Technology™ by Digital Surf (France).

RESULTS AND DISCUSSION

The results of the completed experiments and analyses were presented using the examples of three registered microtopographies obtained from the GWAS: the referential grinding wheel (R) and two grinding wheels with shaped microdiscontinuities (No. 7 and No. 46). The parameters of microtopographies registered using a 3D laser measuring microscope LEXT OLS4000, for selected samples, are presented in Table 4. All of the measurements were taken using a microscopic lens with designation MPLFLN, made by Olympus, whose characteristics are depicted in Table 5. The measuring time was variable and lasted from a few to a few dozen

Table 4: Parameters of Image Acquisition from the Sample Used in Experiments

Lp.	Sample Designation	Scanning Mode	Image Size (pixels)	Image Size (mm)	Type of Objective Lens	Zoom
1	R	XYZ Fast Scan + Color	2868 × 2852	7.189 × 7.149	MPLFLN	1×
2	7		5466 × 1116	23.385 × 4.776*		
3	46		5489 × 1602	16.438 × 4.798*		

Note: * using image stitching procedure.

Table 5: Parameters of MPLFLN Objective Lens

Designation	Producer	Type of Objective Lens	Mag.	NA	WD (mm)	FN (mm)	Imm.
MPLFLN	Olympus	M Plan SemiApochromat	5×	0.15	20.0	26.5	Dry

Note: Mag. – Magnification; NA – Numerical Aperture; WD – Working Distance; FN – Field Number; and Imm. – Multi-immersion

minutes (particularly when including the image stitching procedure).

Figure 3 presents selected views, analyses and parameters of the referential grinding wheel surface texture (R). The top part of Figure 3 shows the real image of a surface sized 7.189 × 7.149 mm and acquired using a brightfield technique in the optical mode, along with a 3D map sized 7.189 × 7.149 × 1.430 mm obtained in the confocal mode. The images were acquired using OLS4000 2.1 software. Under the above-mentioned images the corresponding results obtained using TalyMap Platinum 5.0 software are presented. They include: a 2D surface map of the GWAS, a 2D profile and a 3D surface topography of the GWAS with selected parameters.

When analyzing the images and maps obtained the relative uniformity of the tool active surface, with visible abrasive grain edges of PFA in vitrified bond, can be observed. As the grinding wheel appeared to have no shaped microdiscontinuities, the total height of the leveled surface measured, was *St* = 0.601 mm, which adhered to the technical characteristics of the grinding wheel.

Figure 4 presents collected results for grinding wheel No. 7. In this case the microdiscontinuities were shaped using the abrasive water-jet, with a working pressure of 366.801 MPa. A fragment, sized 15.9 × 4.72 × 1.53 mm, was extracted from the acquired grinding wheel, real image sized 23.300 × 4.760 × 2.380 mm. This fragment is presented in the form of a 3D surface topography for which the values of the selected amplitude (*Sa*, *St*), hybrid (*Sdr*) and spatial (*Sds*) parameters were determined in accordance with (Stout *et al.*, 1993). 3D surface topography was also used in determining a single 2D profile, which allowed for precise analysis of the microdiscontinuity shaping. As in the case of 3D surface topography, the values of the selected 2D parameters were determined (*Ra*, *Rq*, *Rp*, *Rv*, *Rt*, *Rsk* and *Rku*). Geometrical analysis connected with the determination of the maximum depth volume and surface area of the obtained microdiscontinuities, was also carried out.

Figure 5 presents analogical results of the analyses for grinding wheel No. 46, in which

Figure 3: The Collected Results from the Experiment Carried Out for Reference Sample (R), Performed Using the 3D Laser Measuring Microscope LEXT OLS4000

2D VIEW: 2D IMAGE OF THE GWAS
Objective lens: M Plan SemiApochromat MPLFLN
Producer: Olympus | Mag.: 5× | Zoom: 1×
Observation technique: brightfield (true colors)

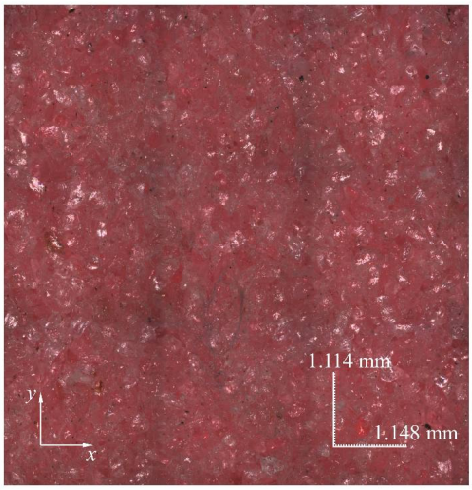

3D VIEW: AXONOMETRIC MAP OF THE GWAS
Objective lens: M Plan SemiApochromat MPLFLN | Producer: Olympus | Mag.: 5×
Zoom: 1× | Observation technique: confocal | Visualization mode: color 3D height map (true colors) | Software: OLS4000 2.1

Surface dimensions (*x*, *y*, *z* axes):
7.189 × 7.149 × 1.430 mm
Measurement time: 8626 s

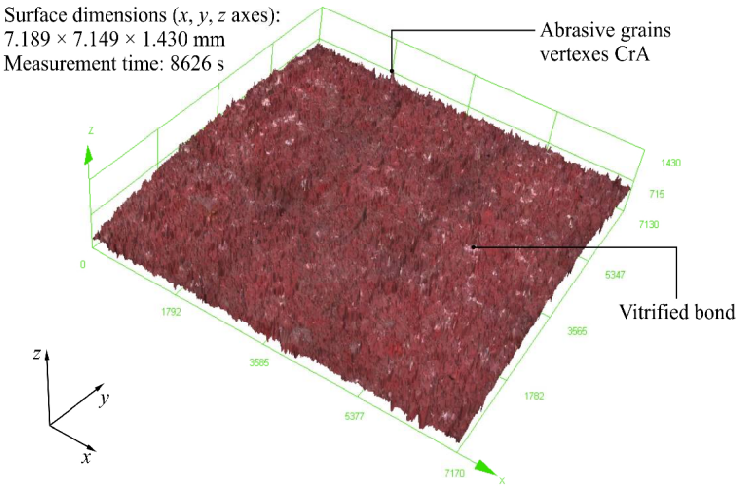

2D VIEW: 2D CONTOUR MAP OF THE GWAS
Visualization mode: color contour map after leveling (simulated colors) | Software: TalyMap Platinum 5.0

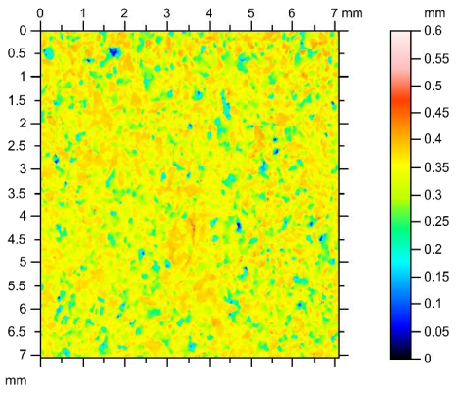

3D VIEW: AXONOMETRIC IMAGE OF THE GWAS TOPOGRAPHY
Visualization mode: color surface topography (simulated colors)
Software: TalyMap Platinum 5.0

Surface dimensions (*x*, *y*, *z* axes): 7.090 × 7.050 × 0.600 mm
Number of points of a single profile (*x* | *y* axes): 2868 | 2852
Spacing between single profiles (*x* | *y* axes): 0.0025 mm | 0.0025 mm
Vertical resolution
(*z* axis): 0.000028 mm

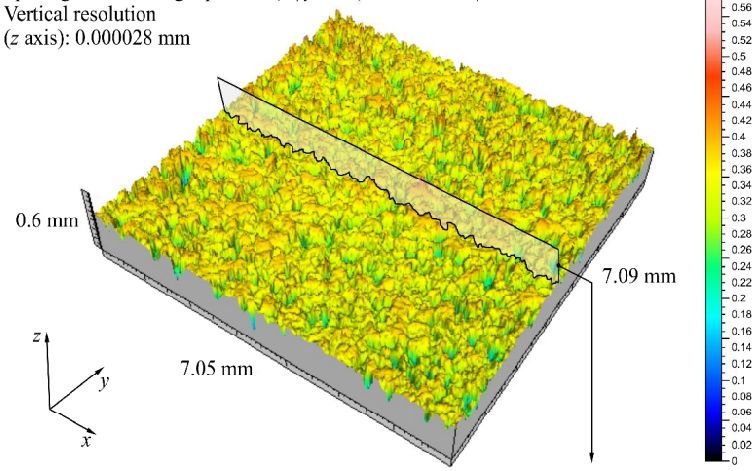

SELECTED TEXTURE PARAMETERS OF THE GWAS

Sa = 0.0324 mm
St = 0.601 mm
Sdr = 203%
Sds = 98.7 1/mm^2

SELECTED ROUGHNESS PROFILE PARAMETERS OF THE GWAS

Ra = 0.0185 mm
Rq = 0.0225 mm
Rp = 0.0337 mm
Rv = 0.0513 mm
Rt = 0.147 mm
Rsk = -1,26
Rku = 5.88
Rz = 0.085 mm

2D VIEW: EXTRACTED A SINGLE PROFILE OF THE GWAS

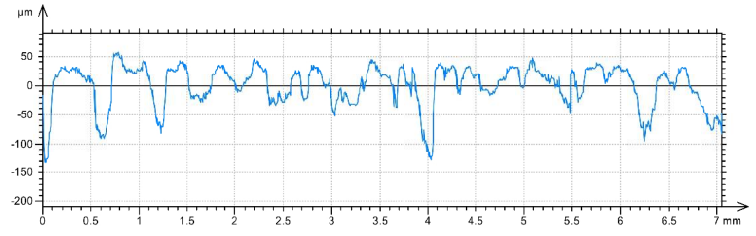

Figure 4: The Collected Results from the Experiment Carried Out on Sample No. 7, Performed Using the 3D Laser Measuring Microscope LEXT OLS4000

2D VIEW: 2D IMAGE OF THE GWAS
Objective lens: M Plan SemiApochromat MPLFLN | Producer: Olympus | Mag.: 5× | Zoom: 1×
Observation technique: brightfield (true colors)

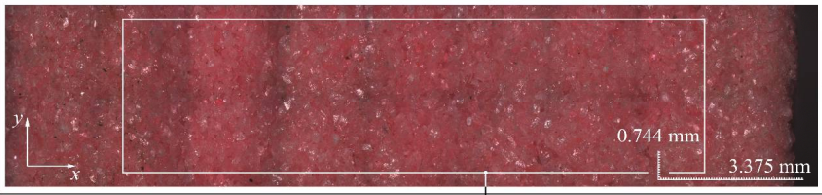

2D VIEW: 2D CONTOUR MAP OF THE GWAS
Visualization mode: color contour map (simulated colors) Software: TalyMap Platinum 5.0

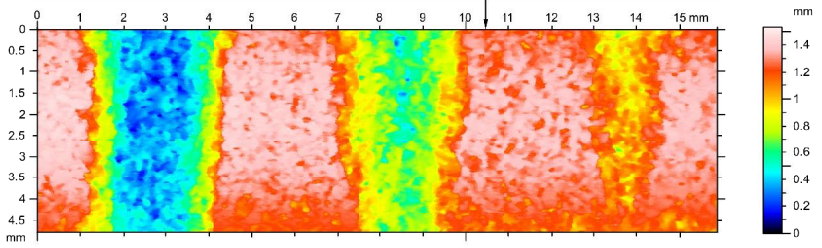

SAMPLE SHORT CHARACTERISTICS

Sample No. 7
Microdiscontinuities shaped using an abrasive water-jet, with a working preassure of 366.801 M1Pa

SELECTED ROUGHNESS PROFILE PARAMETERS OF THE GWAS

$Ra = 0.0308$ mm
$Rq = 0.0403$ mm
$Rp = 0.071$ mm
$Rv = 0.0976$ mm
$Rt = 0.318$ mm
$Rsk = -0.762$
$Rku = 5.59$
$Rz = 0.169$ mm

SELECTED TEXTURE PARAMETERS OF THE GWAS

$Sq = 0.288$ mm
$St = 1.541$ mm
$Sdr = 730\%$
$Sds = 97.0$ 1/mm^2

3D VIEW: AXONOMETRIC MAP AND TOPOGRAPHY OF THE GWAS

3D VIEW: AXONOMETRIC MAP OF THE GWAS
Objective lens: M Plan SemiApochromat MPLFLN
Producer: Olympus | Mag.: 5× | Zoom: 1× | Observation technique: confocal | Visualization mode: color 3D height map (true colors) | Software: OLS4000 2.1
Measurement time: 2796 s

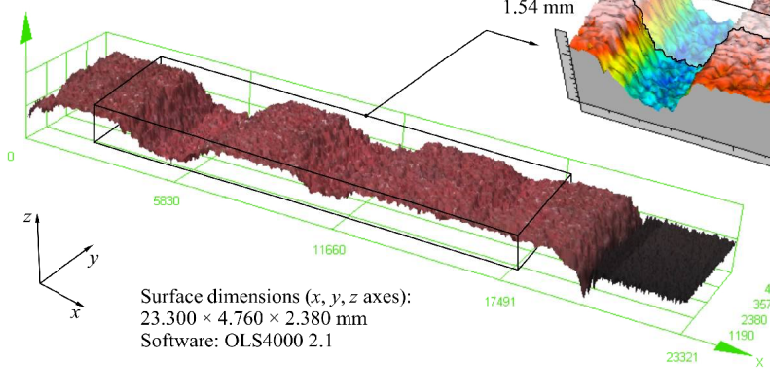

Surface dimensions (x, y, z axes):
23.300 × 4.760 × 2.380 mm
Software: OLS4000 2.1

3D VIEW: AXONOMETRIC IMAGE OF THE GWAS TOPOGRAPHY
Visualization mode: color surface topography (simulated colors)
Number of points of a single profile (x | y axes): 1016 | 1016
Spacing between single profiles (x | y axes): 0.0156 mm | 0.00465 mm
Vertical resolution (z axis): 0.001 mm
Software: TalyMap Platinum 5.0

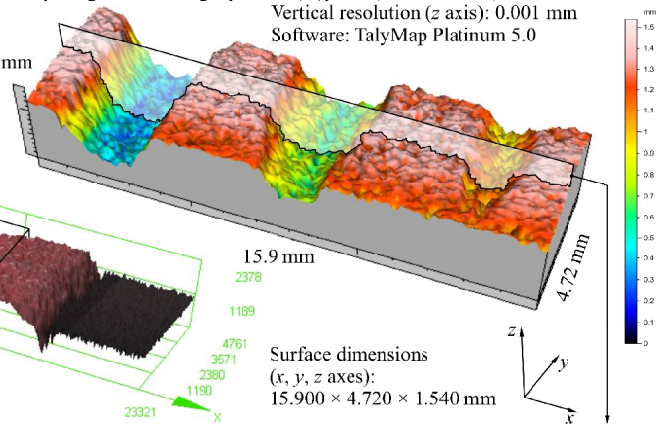

Surface dimensions (x, y, z axes):
15.900 × 4.720 × 1.540 mm

2D VIEW: EXTRACTED A SINGLE PROFILE OF THE GWAS AND RESULTS OF GEOMETRICAL ANALYSIS OF THE MICRODISCONTINUITIES (width, depth and hole surface measurement)

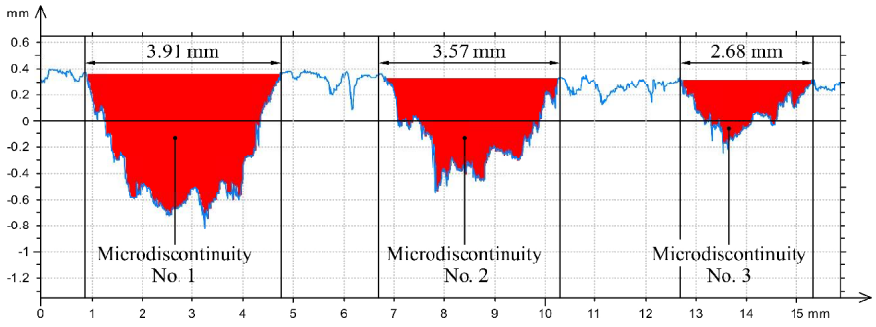

Microdiscontinuity No. 1
Maximum depth: 1.200 mm
Area of the hole: 2.840 mm^2

Microdiscontinuity No. 2
Maximum depth: 0.887 mm
Area of the hole: 1.690 mm^2

Microdiscontinuity No. 3
Maximum depth: 0.561 mm
Area of the hole: 0.699 mm^2

Figure 5: The Collected Results from the Experiment Carried Out for Sample No. 46, Performed Using the 3D Laser Measuring Microscope LEXT OLS4000

2D VIEW: 2D IMAGE OF THE GWAS
Objective lens: M Plan SemiApochromat MPLFLN | Producer: Olympus | Mag.: 5× | Zoom: 1×
Observation technique: brightfield (true colors)

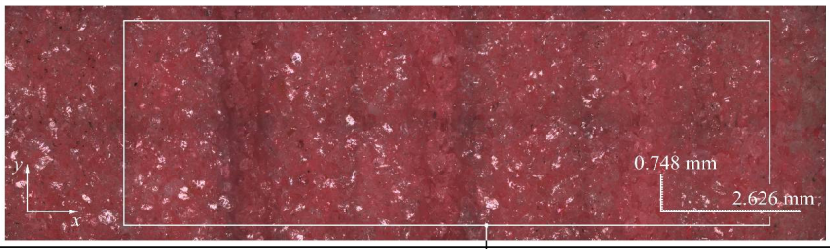

2D VIEW: 2D CONTOUR MAP OF THE GWAS
Visualization mode: color contour map (simulated colors) | Software: TalyMap Platinum 5.0

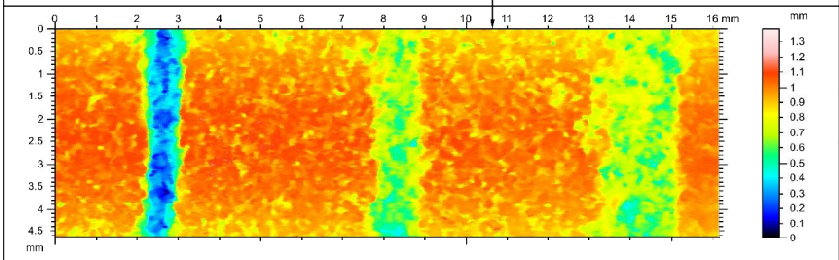

SAMPLE SHORT CHARACTERISTICS

Sample No. 46
Microdiscontinuities shaped using a water-jet, with a working preassure of 124.105 MPa

SELECTED ROUGHNESS PROFILE PARAMETERS OF THE GWAS

Ra = 0.0315 mm
Rq = 0.0412 mm
Rp = 0.0747 mm
Rv = 0.0961 mm
Rt = 0.436 mm
Rsk = 0.16
Rku = 11.6
Rz = 0.171 mm

SELECTED TEXTURE PARAMETERS OF THE GWAS

Sq = 0.136 mm
St = 1.390 mm
Sdr = 890%
Sds = 104.0 1/mm^2

3D VIEW: AXONOMETRIC MAP AND TOPOGRAPHY OF THE GWAS

3D VIEW: AXONOMETRIC MAP OF THE GWAS
Objective lens: M Plan SemiApochromat MPLFLN
Producer: Olympus | Mag.: 5× | Zoom: 1× | Observation technique: confocal | Visualization mode: color 3D height map (true colors) | Software: OLS4000 2.1
Measurement time: 2244 s

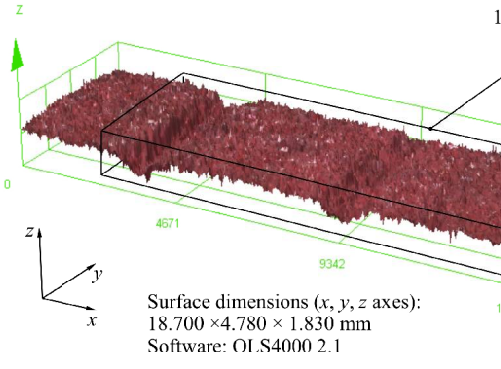

3D VIEW: AXONOMETRIC IMAGE OF THE GWAS TOPOGRAPHY
Visualization mode: color surface topography (simulated colors)
Number of points of a single profile (x | y axes): 1016 | 1016
Spacing between single profiles (x | y axes): 0.0159 mm | 0.00457 mm
Vertical resolution (z axis): 0.001 mm
Software: TalyMap Platinum 5.0

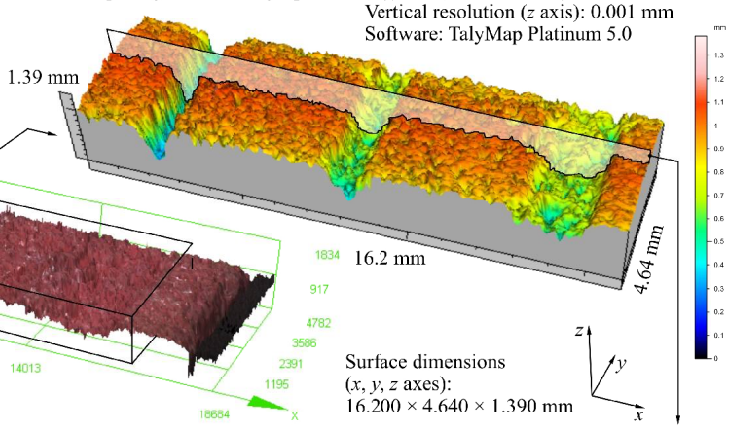

2D VIEW: EXTRACTED A SINGLE PROFILE OF THE GWAS AND RESULTS OF GEOMETRICAL ANALYSIS OF THE MICRODISCONTINUITIES (width, depth and hole surface measurement)

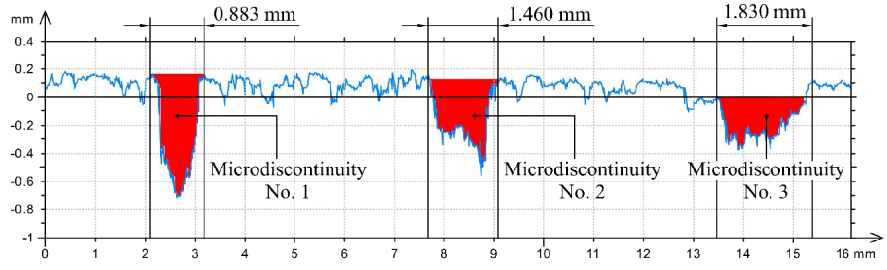

Microdiscontinuity No. 1
Maximum depth: 0.875 mm
Area of the hole: 0.534 mm^2

Microdiscontinuity No. 2
Maximum depth: 0.693 mm
Area of the hole: 0.473 mm^2

Microdiscontinuity No. 3
Maximum depth: 0.378 mm
Area of the hole: 0.400 mm^2

discontinuities were shaped with a low working pressure (124.105 MPa), without the use of abrasives.

The greater energy of the abrasive water-jet used in the case of grinding wheel No. 7, resulted in shaping discontinuities characterized by a 1.75 (the smallest discontinuity) to a 5.31 (the biggest discontinuity) times bigger cross-sectional area, when compared to grinding wheel No. 46. The discontinuity depth resulted mostly from the position of the machining head and was not considerably different in both cases. The largest recorded difference was approximately 37% in the case of the deepest microdiscontinuity. On the other hand, the microdiscontinuities widths are diametrically opposed. In the case of the grinding wheel shaped with a high-pressure abrasive water-jet (Figure 4), the microdiscontinuity width ranged from approximately 4.42 to 1.46 times greater than the width of the microdiscontinuities shaped with the water-jet with a pressure of 124.105 MPa (Figure 5). Shaping microdiscontinuities on the GWAS led to an increase in the number of free intergranular spaces, as well as a considerable increase in the total height of the unevenness of the obtained surface. In the case of the referential grinding wheel the value of the St parameter was 0.601 mm, while in the case of grinding wheel No. 7 St = 1.541, and with grinding wheel No. 46 St = 1.390. This translates to over a two-fold increase of this parameter (256% for grinding wheel No. 7 and 231% for grinding wheel No. 46). A comparison of the obtained measurement results for all of the examined samples is presented, in the form of diagrams, in Figure 6.

Figure 6: The Collected Results for the Measurements Pertaining to the Geometrical Parameters of the Microdiscontinuities for All Tested Samples

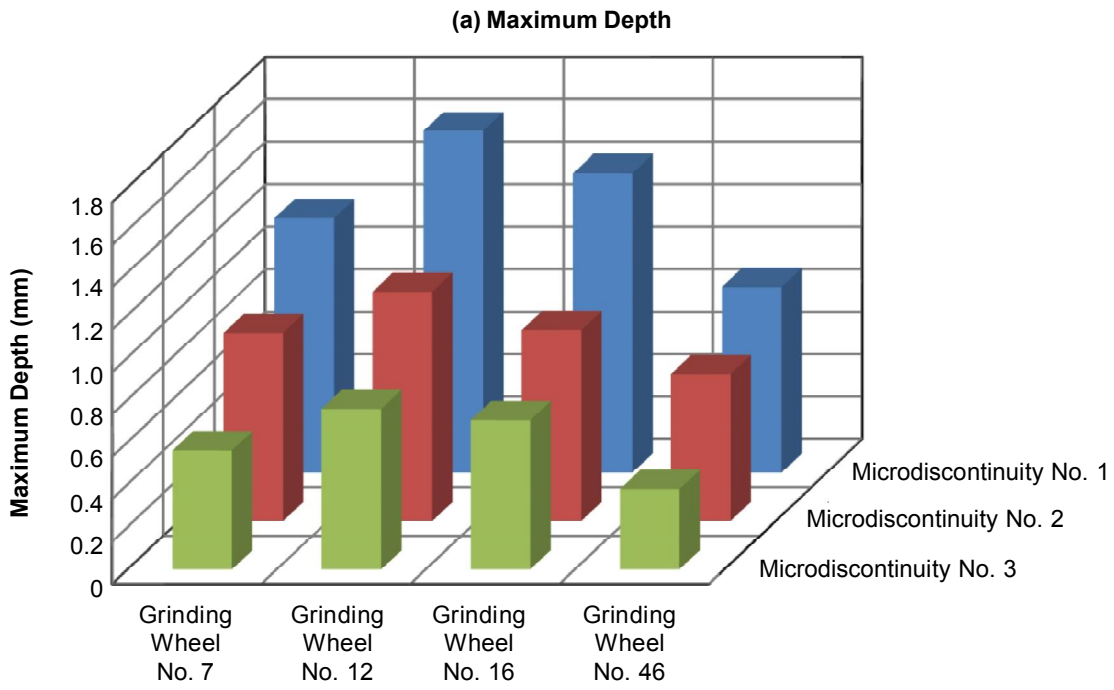

Figure 6 (Cont.)

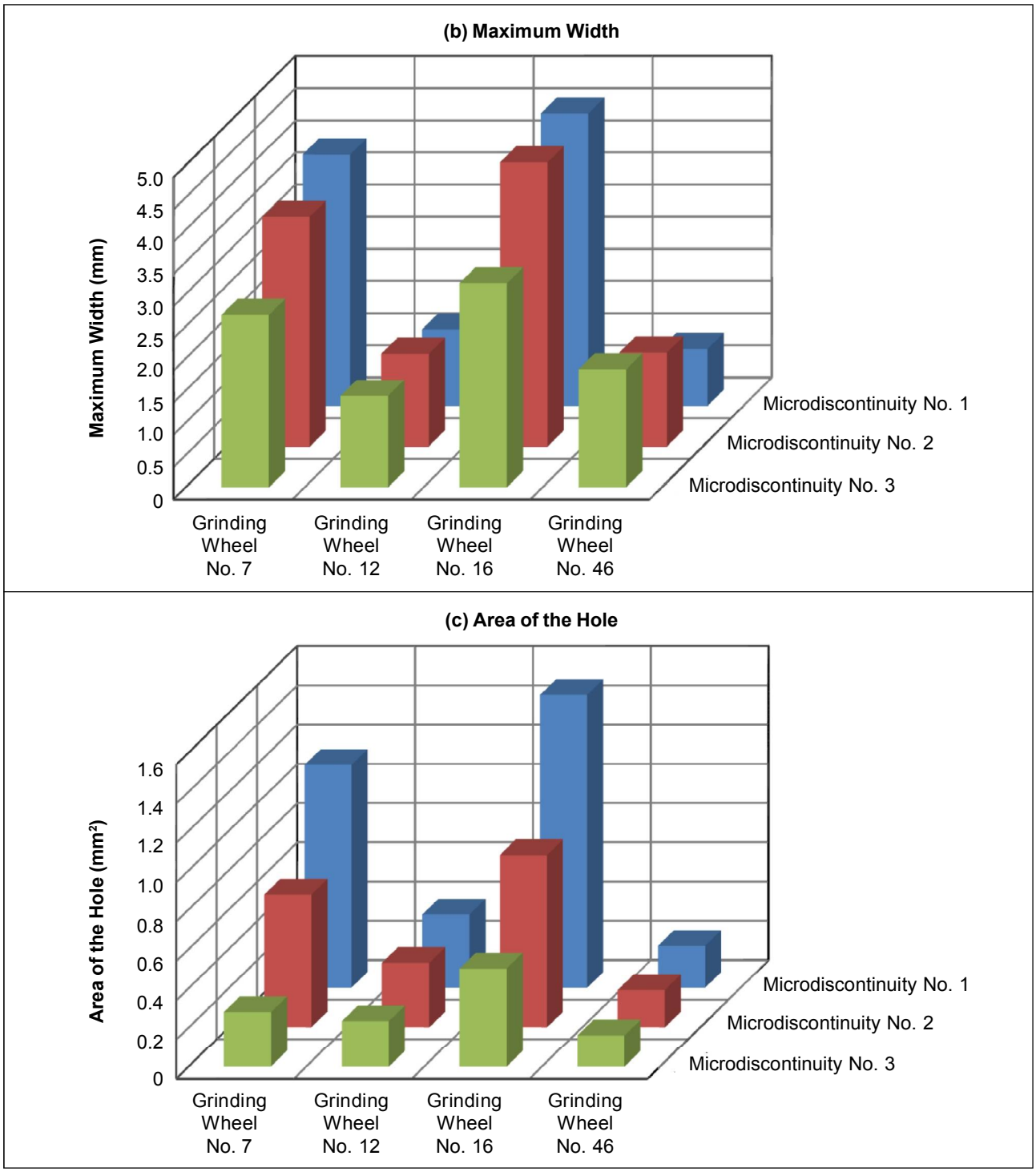

Having analyzed the measurement results obtained, it may be concluded that a change of such high-energy abrasive water-jet parameters, allows for effective steering, with the additional pressure and participation of the abrasives, which results in an improved removal process when shaping the GWAS with PFA grains and vitrified bond. By

maintaining constant machining time grinding wheel discontinuities of various width and cross- sectional area can be obtained. These geometrical features of the discontinuities are of decisive functional meaning, as the volume of the additional shaped intergranular spaces, whose presence influences the grinding process in a positive way, is contingent upon them. A comparison of the width value and areas of the discontinuities shaped with the water-jet and the abrasive water-jet, proves decisively that the addition of abrasives to the water-jet exerted the greatest influence upon their geometry (Figures 6b and 6c).

The experiment results obtained (Figures 3-5) also prove the high usability of the CLSM as a measurement technique in the assessment of abrasive tools surfaces, modified in the above-described ways.

CONCLUSION

The article presents possible applications of CLSM in the assessment of the condition of the GWAS with PFA grains and vitrified bond. The grinding wheels examined underwent the procedure of shaping microdiscontinuities using high-pressure abrasive water-jets with various technological parameters. The results obtained from measurement of the GWAS in this manner, confirmed the high usability of the measurement method described.

The obtained surface microtopographies allowed for a thorough visual and parametrical analysis of the assessed grinding wheels. On the basis of this analysis, it was concluded that the application of a high-energy abrasive water-jet (with a pressure of 366.801 MPa) facilitated shaping discontinuities of greater width and cross- sectional area than in the case of a low-pressure water-jet (with a pressure of 124.105 MPa).

The CLSM technique may constitute an interesting alternative for methods currently used in abrasive tools diagnostics, such as stylus and optical profilometry, as well as interference microscopy. It may also complement the above methods as a referential method. In years to come Confocal should be expected to become one of the most rapidly developing and exceptionally dynamic optical measurement techniques. Already today there are numerous science and technology areas where it is used extensively.

ACKNOWLEDGMENT

Part of this work was supported by the Polish Ministry of Science and Higher Education under Grant No. N503 214837. The Authors would like to thank Mrs. Daniela Herman, D.Sc, Ph.D., from the Division of Fundamentals of Materials Science of the Institute of Mechatronics, Nanotechnology and Vacuum Technique at Koszalin University of Technology, for preparing the grinding wheels for tests, Mr. Michal Bielecki, M.Sc., B.Sc., from Unconventional HydroJetting Technology Center at Koszalin University of Technology, for shaping of the microdiscontinuities on the GWAS, as well as Mr. Robert Tomkowski, M.Sc., B.Sc., from the Laboratory of Micro- and Nanoengineering at Koszalin University of Technology, for the optical m measurement of the test samples surface topographies.

REFERENCES

1. Amos W B and White J G (2003), “How the Confocal Laser Scanning Microscope Entered Biological Research”, *Biology of the Cell*, Vol. 95, No. 6, pp. 335-342.

2. ANSI B74.12-2009 (2009), "Specifications for the Size of Abrasive Grain – Grinding Wheels, Polishing and General Industrial Uses", American National Standards Institute, New York.
3. Brakenhoff G J, Blom P and Barends P (1979), "Confocal Scanning Microscopy with High-Aperture Lenses", *Journal of Microscopy*, Vol. 117, No. 2, pp. 219-232.
4. Buzug T M (2008), "Computed Tomography: From Photon Statistics to Modern Cone-Beam CT", Springer-Verlag.
5. Chen J, Moschakis T and Pugnaloni L A (2006), "Surface Topography of Heat-Set Whey Protein Gels by Confocal Laser Scanning Microscopy", *Food Hydrocolloids*, Vol. 20, No. 4, pp. 468-474.
6. Cierniak R (2011), "X-Ray Computed Tomography in Biomedical Engineering", Springer-Verlag.
7. Clarke A R and Eberhardt C N (2002), "Microscopy Techniques for Materials Science", CRC Press.
8. Claxton N S, Fellers T J and Davidson M W (2010), "Laser Scanning Confocal Microscopy", available at http://www.olympusfluoview.com/theory/LSCMIntro.pdf
9. Conn P M (Ed.) (2010), "Techniques in Confocal Microscopy", Elsevier.
10. Evans A A and Donahue R E (2008), "Laser Scanning Confocal Microscopy: A Potential Technique for the Study of Lithic Microwear", *Journal of Archaeological Science*, Vol. 35, No. 8, pp. 2223-2230.
11. Favretto S (2007), "Applications of X-ray Computed Microtomography to Materials Science", VDM Verlag.
12. FEPA 42-1:2006 (2006), "Grains of Fused Aluminium Oxide, Silicon Carbide and Other Abrasive Materials for Bonded Abrasives and for General Applications Macrogrits F4 to F220", Federation of European Producers of Abrasives, Paris.
13. Hsieh J (2003), "Computed Tomography: Principles, Design, Artifacts, and Recent Advances", SPIE Press Monograph, PM114, SPIE.
14. ISO 8486-1:1996 (1996), "Bonded Abrasives – Determination and Designation of Grain Size Distribution – Part 1: Macrogrits F4 to F220", International Organization for Standardization, Geneva.
15. Jones C W, Smolinski D, Keogh A, Kirk T B and Zheng M H (2005), "Confocal Laser Scanning Microscopy in Orthopaedic Research", *Progress in Histochemistry and Cytochemistry*, Vol. 40, No. 1, pp. 1-71.
16. Kalender W A (2011), "Computed Tomography: Fundamentals, System Technology, Image Quality, Applications", Publicis Corporate Publishing, Erlangen.
17. Mahmoud T, Tamaki J and Yan J (2003), "Three-Dimensional Shape Modeling of Diamond Abrasive Grains Measured by a Scanning Laser Microscope", *Key Engineering Materials*, Vols. 238-239, pp. 131-136.
18. Miao Z-J, Shan A-D, Wang W, Lu J, Xu W-L and Song H-W (2011), "Solidification Process of Conventional Superalloy by

Confocal Scanning Laser Microscope", *Transactions of Nonferrous Metals Society in China*, Vol. 21, No. 2, pp. 236-242.

19. Midgley P A, Ward E P W, Hungría A B and Thomas J M (2007), "Nanotomography in the Chemical, Biological and Materials Sciences", *Chemical Society Reviews*, Vol. 36, No. 9, pp. 1477-1494.
20. Miller F P, Vandome A F and McBrewster J (2010), "Confocal Laser Scanning Microscopy", Alphascript Publishing.
21. Minsky M (1957), US Patent No. 3013467.
22. Minsky M (1988), "Memoir on Inventing the Confocal Scanning Microscope", *Scanning*, Vol. 10, No. 4, pp. 128-138.
23. Nadolny K and Kaplonek W (2012), "Design of a Device for Precision Shaping of the Grinding Wheel Macro- and Microgeometry", *Journal of Central South University of Technology*, Vol. 19, No. 1, pp. 135-143.
24. Pawley J B (Ed.) (2006), *Handbook of Biological Confocal Microscopy*, 3rd Edition, Springer Science+Buisness.
25. Plichta J and Bil T (1992), "Method of Grinding Wheel Dressing Using Single-Grain Dresser", Polish Patent No. 155182.
26. Price R L and Jerome W G (Eds.) (2011), "Basic Confocal Microscopy", Springer Science+Business Media.
27. Publication No. EUR 15178 EN (Final Report) BCR, European Community, Brussels.
28. Stout K J, Sullivan P J, Dong W P, Mainsah E, Lou N, Mathia T and Zahouani H (1993), "The Development of Methods for the Characterization of Roughness in Three Dimensions".
29. Surhone L M, Tennoe M T and Henssonow S F (2011), *Nanotomography*, Betascript Publishing.

APPENDIX

NOMENCLATURE

Ra	Arithmetic mean deviation of profile, mm
Rq	Root mean square deviation of profile, mm
Rp	Maximum profile peak height, mm
Rv	Maximum profile valley depth, mm
Rt	Total height of profile, mm
Rz	Maximum height of profile, mm
Rsk	Skewness of profile, –
Rku	Kurtosis of profile, –
Sa	Arithmetic mean height, mm
St	Total height of the surface, mm
Sdr	Developed interfacial area ratio, %
Sds	Density of summits of the surface, $1/mm^2$

ABBREVIATIONS

ANSI	American National Standards Institute
CLSM	Confocal Laser Scanning Microscope
FEPA	Federation of European Producers of Abrasives
GWAS	Grinding Wheel Active Surface
ISO	International Organization for Standardization
PFA	Pink Fused Alumina